Lab on a Chip

Accepted Manuscript

ROYAL SOCIETY OF CHEMISTRY

www.rsc.org/loc

Fine structuration of low-temperature co-fired ceramic (LTCC) microreactors

Bo Jiang[a&b*], Julien Haber[c], Albert Renken[c], Paul Muralt[a], Lioubov Kiwi[c] and Thomas Maeder[b*]

[a]Ceramics Laboratory EPFL, Lausanne, Switzerland
[b]Laboratory of Microengineering for Manufacturing EPFL, Lausanne, Switzerland
[c]Group of Catalytic Reaction Engineering EPFL, Lausanne, Switzerland

Abstract

The development of microreactors that are operating under harsh conditions is always of great interests for many applications. Here we present a microfabrication process based on low-temperature co-fired ceramic (LTCC) technology for producing microreactors, which are able to perform chemical processes at elevated temperature (> 400°C) and against concentrate harsh chemicals such as sodium hydroxide, sulfuric acid and hydrochloric acid. Various micro-scale cavities and/or fluidic channels are successfully fabricated in these microreactors, using a set of combined and optimized LTCC manufacturing processes. Among them, it has been found that the laser micromachining and the multi-step low-pressure lamination are particularly critical to the fabrication and quality of these microreactors. Demonstration of LTCC microreactors with various embedded fluidic structures are illustrated with a number of examples, including micro-mixers for studies of exothermic reactions, multiple-injections microreactors for ionones production, and high-temperature microreactors for portable hydrogen generation.

Keywords: LTCC, microreactor, structuration, harsh environment

*Corresponding authors: Bo Jiang, bo.jiang@empa.ch; Thomas Maeder, thomas.maeder@epfl.ch

Introduction

Chemical microreactors are type of meso-scaled reaction systems that have a characteristic dimension of fluidic channels in the sub-millimeter range. Combining process intensification concepts with microfabrication techniques, these microreactors have been rapidly developed to perform liquid - / gas - phase chemical reactions, particularly for these quasi-instantaneous endothermic or exothermic ones[1, 2]. Ceramic materials in general feature high chemical and thermal stability. Hence they are very preferable to be used as reactor construction materials, especially for these reactors involving with high temperature and/or harsh chemical reactions[3-10]. Knitter et al.[3] has demonstrated alumina-based reactors using an injection molding process, in which molds were fabricated through a stereolithography method. These reactors contain various micro-scale fluidic structures and can be applied up to 1100°C. Meschke and his team[5] have developed a microchannel fabrication process based on laser machining or milling for producing silicon carbide (SiC) based reactors. Comparing to alumina and SiC, from aspect of material properties, fired LTCC devices has a relatively low operating temperature that is feasible for any process below 800°C[11]; and they show good resistance to certain kinds of aggressive wet chemicals[12]. More important, the LTCC technology - a multiple layer based manufacturing method - exhibits several advantages over other ceramic fabrication processes. LTCC is very compatible with thick-film technology: having very similar peak processing temperature, usually in the range of 850°C – 900°C, thick-film conductive or resistive materials are able to be either screen printed on LTCC green tapes and fired together at one-step manufacturing (“co-fired”), directly fabricated on fired LTCC ("post-fired")[13]. It consequently promotes the integration ability of electronic components into LTCC devices, such as sensors, actuators and electrical packaging, for realizing accurate process control and real-time automation[14, 15]. Another advantage of LTCC for making microreactors is that their green tapes appear flexible and can be easily machined for creating cavities via milling[16], embossing[17], laser cutting[18], and sacrificial materials[19]. Through stacking and laminating these green tapes with cavities in 3D, these stacks can incorporate various embedded or open fluidic structures in the sub-mm scale for desired chemical processes, to name a few, packed-bed[20], microchannels[9], heat exchangers[21] and mixers[22]. Besides, LTCC technology is a low-cost manufacturing method, and requires less investment and maintenance cost than silicon-based microfabrication one, making it suited for both high-volume production and fast prototyping cycles.

Incorporating fluidic structures into LTCC microreactors primarily depends on its lamination process. Standard ones (isostatic or uniaxial thermocompression) cannot be used, as the embedded fluidic structures (e.g. channels or cavities) get easily damaged in the stacked LTCC tapes by the high lamination temperature and/or pressure, causing sagging, tearing and cracking issues. Several approaches have been proposed so far in order to reduce these deformations and improve quality of integrated LTCC fluidic structures. One method is using temporary inserts to introduce mechanical supports to the LTCC cavities for avoiding the deformation and/or sagging during the lamination. These inserts, usually solid flexible objects[23], are removed right after the lamination. However, the removal of inserts from the laminate can cause permanent damage to these fluidic structures. Besides, this method is not applicable for fabricating fully embedded fluidic channels.

Alternatively, a chemical-assisted lamination process has been proposed to provide a low-pressure and/or low-temperature bonding of LTCC green tapes. Roosen et al.[24] has used double-side adhesive tapes that contain acrylate adhesives and a poly-ethylene terephthalate (PET) film to ensure a temporary binding of green tapes under a low lamination pressure at the ambient temperature. Upon heating (40°C – 60°C), these adhesives, together with the binders in the LTCC green tapes, soften and join the laminates by their capillary forces. Except using adhesives, chemical solvents are also used for providing temporary gluing of LTCC green tapes at low pressure and room temperature[18, 25]. These solvents are usually some of the organic compositions in LTCC green tapes or thick-film materials. Although these methods are proven to achieve sustainable LTCC cavities with very minimal deformation, their process reliability can be a potential issue involving with integrating thick-film materials or electrical via. On the other hand, these binding agents introduce additional organic contents into LTCC laminates and exacerbate their debinding process during firing[26], which eventually increases the manufacturing lead time and cost.

Another solution is to use sacrificial volume materials (SVM). These SVM are placed into the stacked LTCC tapes to provide mechanical supports as well as prevent the embedded fluidic channels from collapsing and/or deformation during the lamination and/or firing process. Common SVM are carbon-based fugitive materials[27, 28], which nominally burn out from LTCC samples between debinding and sintering stages. Organic SVM are also used such as waxes and polymers[18, 29], which burn out only at the debinding step. The drawback of using SVM is its extended firing time, increasing manufacturing cost largely. Moreover the SVM residual in the fluidic channels, which are left in the device due to improper burnt-out process, can contaminate the carried reactions and/or installed catalyst, hindering the microreactor's performance.

The reference review above has clearly shown current limitations on fabricating embedded fluidic structure in LTCC-based microreactors. To overcome these issues, we present a simple and reliable microfabrication strategy for developing LTCC-based microreactors with integrated fine and complex fluidic structures. The proposed process is a combination of a laser micromaching, a multi-steps lamination, and a firing process. In order to produce LTCC microreactors with intact fluidic structure, various optimization studies of these processes have been carried out in this work. The optimized microfabrication not only enabled us to incorporate complex fluidic structure into microreactors but also granted us wide opportunities of developing LTCC microreactors in application of harsh chemical process. Using our developed microfabrication process, several novel LTCC microreactors in the range of mm to sub-mm are demonstrated here, including micro-mixers for studying chemical reactions with fast intrinsic kinetics and high exothermicity; multi-injections microreactors for ionones production; and multi-functional high-temperature microreactors for on-site hydrogen production.

Experimental

Stability test

In order to perform reactions of harsh chemicals, LTCC's material stability must be qualified at first. To do so, fired LTCC samples were observed in terms of their etching behavior in several kinds of

chemically aggressive aqueous solutions. Used LTCC were 951 Green Tape™ (DP951, DuPont USA) and Heralock® 2000 (HL2K, Heraeus Germany). DP951 is a conventional LTCC material made of calcium alumosilicate glass and alumina fillers that has a planar shrinkage of **12.7% (X- and Y- axis)** after firing[30]. HL2K, on the other hand, has a more complex three-layer structure, in which the refractory ceramic layer is sandwiched with outer layers rich in glass phase. Upon firing, these layers constrain mutually to have HL2K a nearly zero fired planar shrinkage[31]. In the material stability evaluation, 3 pieces of LTCC green tapes for each kind were cut into a size of 10 × 20 mm^2, laminated and fired under standard manufacturing conditions[32, 33]. The thickness of fired DP951 and HL2K samples were 0.29 mm and 0.27 mm, respectively. Standard alumina pieces (grade 96%, thickness: 1.0 mm, Haldemann & Porret SA, Switzerland) with similar size were used for the test as references. The tested chemicals included 2.0 $mol \cdot L^{-1}$ sodium hydroxide (NaOH), 9.1$mol \cdot L^{-1}$ of sulfuric acid in water (H_2SO_4) and 0.2 $mol \cdot L^{-1}$ hydrochloric acid in water (HCl). These wet chemicals with defined concentrations are commonly used in industrial chemical reactions[2]. The concentrated sodium hydroxide solution was additionally used to investigate the leaching stability of LTCC materials, as the silicate-based glass content in LTCC was very soluble in this condition[13]. The weight loss of LTCC and alumina samples, stored at room temperature, was measured after 1, 2 and 4 weeks. The chemical stability of all tested samples were compared in terms of a cumulative weight loss (ΔW), normalized to the surface area of tested samples as defined in Equation 1.

Laser micromachining of LTCC fluidic structure

Laser micromachining is widely considered as one of the most versatile methods for structuring fluidic cavities in individual LTCC green tapes, at least for prototypes or small series production. This is mainly because of its fine structuration resolution, absence of mechanical contact with tape surface for minimal contamination, and high processing speed . In this work, the laser structuration took place by a diode pumped Nd:YAG trimming laser source (LS9000, wavelength 1064 nm, power output 3 W, spot size 50 µm, Laser Systems Germany) equipped with a computer-controlled galvanometric beam deflection system. The laser beam with wavelength of 1064 nm has been generally identified suited for machining LTCC green tapes[34, 35]. A herringbone structure served for this study. The structure contained several parallel groove frameworks (100 µm wide) in a 500 µm wide fluidic channel. Several process dependences of the machining quality in LTCC green tapes were evaluated, including diode power, I [W], frequency of the optical switch, f [kHz], and velocity of beam deflection, v [$mm \cdot s^{-1}$]. The quality of machined test structures in both HL2K (tape thickness: 133 µm) and DP951 (tape thickness: 245 µm) green tapes was examined by an optical microscopy (M165C, Leica Microsystem Inc, Germany).

Multi-step lamination process

In order to fabricate complex embedded fluidic structures with little damage in LTCC devices, we propose a modified uniaxial lamination process. **Figure 1** shows a schematic of our approach, which basically consists of a pre-lamination with standard lamination pressure at room temperature, and a low-pressure lamination at elevated temperature. For the pre-lamination, since all LTCC tapes in these sub-laminates have identical cavities, the standard lamination pressure can be applied without concerns of damaging fluidic structures. Such a step aimed (i) to build up the height of the cavities for the desired aspect ratio of fluidic channels; (ii) to increase overall thickness of these sub-

laminates for enforced mechanical strength during the low-pressure lamination; (iii) to avoid delamination in the stacks where some multiple layers of LTCC tapes are sandwiched by cavities and receive no lamination pressure at both sides.

The second lamination process, although only one step was shown in **Figure 1** and used for the test, can be made for several stages for the cases with complex fluidic structures. It is expected that the organic binder content in the tapes become soft at elevated temperature to join the stacked sub-laminates properly only by a relatively low compressive pressure. In such a way, the deformation or collapsing of embedded LTCC fluidic structures can be prevented, while the good joining in the stacks is still achievable. It is primarily because the built-up thickness in the sub-laminates improves their mechanical strength and minimizes their deformation during the low-pressure lamination. This method is especially effective in the situation that some multiple layers sub-laminates are sandwiched by cavities from other ones and receive no pressing force during joining.

A similar approach has been mentioned in previous work[36], however, there is no any details available with regard to the lamination process. Specifically it is unknown about optimized lamination processing parameters and their influences on LTCC material variants and fluidic structure complexity. Besides, the feasibility of using such a method in developing LTCC microreactors is still an open question to us. Thus, for the first time, we conducted a more quantitative and comprehensive investigation on optimizing the low-pressure lamination for DP951 and HL2K materials.

The optimization study mainly focused on the second step, the low-pressure lamination. A testing sample was designed for evaluating influences of T and P on the deformation of embedded fluidic channels. Shown in **Figure 2a**, a cavity was cut in DP951 (tape thickness: 245 μm) or HL2K (tape thickness: 133 μm) green tapes by the laser micromachining, having a length of 10 mm and varied width (w) of 0.2 – 1.2 mm. For each kind LTCC, three pieces of these tapes with same cavities were first laminated under lamination pressure, P = 20 MPa, and lamination temperature, T = 25°C. These sub-laminates were then stacked by two blank tapes to embed the cavities (see **Figure 2b**), on which two outgassing lets were made with a diameter of 0.2 mm. The low-pressure lamination was then performed on these stacks by various combinations of T = 40 – 90°C and P= 2 – 8 MPa. A total of 7 lamination conditions were made for the low pressure lamination (see **Table 1**). Three samples were fabricated for each testing condition. Then these prepared laminates were sintered using their standard firing process explained in **Table 2**.

The quality of these embedded fluidic cavities was mainly evaluated by the deflection profile of the suspending LTCC parts over the embedded cavities, in other words, the deformation of the cavity walls, which was achieved an optical profilometer (UBM optical profilometer, 50 nm of optical beam spot size, UBM Corporation Germany). The maximum deflection at such walls after lamination, Δh_1, was defined in Equation 2 (see **Figure 2c**). After firing, these deflections might further develop, of which the profile was unpredictable due to the LTCC shrinkage. It should be noted that these deformations shown in **Figure 2d** were only one of possibilities and the actual case would be known by the profilometric results. We defined the maximum deflection after firing as Δh_2 given by **Equation 3**. In addition, the cross-section of all test samples was evaluated by the optical microscopy.

Results and discussion

Chemical resistance of LTCC materials

The chemical stability of alumina, DP951 and HL2K tapes was examined in the NaOH, H_2SO_4 and HCl solutions by the aging test. Both alumina and DP951 remained the same in their weight and appearance in all tested solutions. Although contained a certain amount of glass phase, DP951 exhibited a very low etching rate (< 0.001 g/mm^2) in the NaOH. By contrast, HL2K showed lower resistance to the NaOH with more weight loss after 4 weeks' aging (~0.064 mg·mm^{-2}). We believe that HL2K's tape structure and composition, especially its contained glass content, certainly affected its chemical stability against the NaOH solution more seriously than others[37].

HL2K composition showed very weak resistance in the acidic environment, as compared with DP951. This is in agreement with previous studies tested in dilute HCl[37], acetic and phosphoric acids[38]. Within 1 week, HL2K samples were totally dissolved in the HCl at room temperature (data not shown). In the case of the H_2SO_4, the ΔW of HL2K ones was about 0.01 mg·mm^{-2} after 4 weeks' aging (see **Figure 3**). The generally poor acid resistance of HL2K agreed with its material studies[31]. They seems to have less severe degradation in the H_2SO_4 than in HCl. HL2K is rich in calcium and lanthanum oxides, such as $CaAl_2B_2O_7$ and $LaBO_3$, and is not supposed to be very acid-resistant [39]. Therefore the formed calcium sulfates ($CaSO_4$) on the surface of HL2K ones had very limited solubility in the H_2SO_4, which actually acted as a passivation layer and prevented the further etching. To further verify our assumption, detailed chemical studies using energy dispersive spectroscopy on the surface of tested HL2K samples will be conducted at next step. Moreover, the tape structure of HL2K is believed to be another explanation for the weak acidic resistance. As Rabe et al. [31] indicated, HL2K is a composite of three layers of ceramic thin tapes sandwiched together, having outer porous layers rich in glassy phase. These outer layers are easy to be reacted with aggressive chemicals and result in fast dissolving especially in HCl, in comparison with DP951 that has a more homogenous structure of mixed glass and refractory materials. Overall, we conclude that DP951 appears more stable in aggressive aqueous chemicals, and hence more suited for microreactor applications

Laser micromachining of LTCC green tapes

Figure 4a depicts the herringbone structure with designed dimension for the laser processing optimization, which contains several parallel groove frameworks, 100 μm wide per each, in a 500 μm wide fluidic channel. Such a test pattern has a structural dimension close to the spot size of our laser beam source and can be an extreme case in the studies. We believe the optimized laser process from this work can be adapted to or directly used for larger scales of green tape micromachining. Generally, the evaluation showed low incident energy were produced by using high *f* and *v* as well as low *I* towards LTCC green tapes and resulted in inefficient melting or removal of DP951 or HL2K materials. These samples led to incomplete cuts or partial removal of materials, for example in DP951 ones as illustrated in **Figure 4d**. By contrast, low *f* and *v* with high *I* generated excessive incident energy into green tapes, resulting in rough and/or burnt edges, bulging cuts, and damaged herringbone structures (see **Figure 4e&f**). Through combining these parameters at optimized levels,

good quality of herringbone structure were achieved in both HL2K (see **Figure 4**b) and DP951 (see **Figure 4**c) cases, in which the I corresponded to 1.2 W, the f and v were 8 kHz and 10 mm·s^{-1}, respectively.

Aside from the laser micromaching, it is believed that good quality of structuration also depends on the kinds of LTCC materials, regarding to their tape structure, absorption coefficient, and thermal conductivity. This was seen from the comparison of cut herringbones between HL2K and DP951 (see **Figure 4b&c**). There were more burnt and ragged edge under identical process conditions in the HL2K, through it (133 μm) was slightly thicker than DP951 (113 μm) though. We suggest that the porous and glassy outer layers in HL2K samples are mainly responsible for this difference, which seems to be melted easier by the laser versus the DP951 one, which has a mesoscopically homogenous mixture of glass, ceramic and organic materials[40].

Multi-step lamination process

Figure 5 shows maximum deflections of embedded cavities with varied w in DP951 and HL2K samples, which were formed during the secondary lamination (Δh_1) and firing (Δh_2) stages under various conditions of T and P. These deformations under same conditions generally had a deviation of ± 0.5 μm, which was mostly due to inherent variation of the lamination process and/or errors of the profilometric measurement. Nevertheless, these results showed a clear trend in the both DP951 and HL2K cases that the deflection of embedded cavity walls was developed with increasing T, P and w.

As seen from **Figure 5a, c,e&g**, For both, it was generally observed a sunken surface at the walls of embedded cavities after the lamination process. HL2K samples generally deformed more than DP951 ones, indicating its cavity walls had less mechanical strength against the lamination process. One may argue this was due to its thinner cavity walls that HL2K ones had (133 μm in green state) as compared with DP951 (254 μm in green state). We then compared both samples made under identical conditions with similar thickness of cavity walls for HL2K (266 μm) and DP951 (254 μm) in green state. Same trend in deformation was found **(see Figure S1 in the supplemental information)**. With increasing T, shown in **Figure 5a&e**, the deflection change in HL2K was more dramatic than that in the DP951 ones. This may indicate that the more deformed HL2K samples was caused its contained organic binders, which behaved quite differently in contrast with DP951[41]. As T increased, these organic binders in the stacked LTCC green tapes became less viscous, interpenetrated into tapes at their interface, and promoted a good joining for the laminates. However, this made the tapes mechanically weak, especially for the cavity walls with mechanical supports that were sensitive to externally applied forces and easily became deformed, leading to sagging or even collapse. High T, large P and W were found to have promoted these deformations. Hence, lamination conditions, geometry of embedded cavities, thickness of cavity walls and types of used LTCC materials must be considered carefully in order to achieve good quality of embedded fluidic structure.

LTCC firing process is another critical step to the quality of these embedded cavities, as the capillary force of melted glass phase in the laminates and their physical shrinkage at the planar direction can deform or even destroy the embedded fluidic structure[23, 42]. Both DP951 and HL2k samples,

laminated under varied T and P, were sintered under their standard firing profile, respectively (see Table 2). Interestingly, the results showed very different ways of these deformations between two kinds of LTCC (see **Figure 5b,d,f&h**). In the case of DP951, the deformation appeared to be reduced largely after firing. A negative value of deflection was even found for these cavities with $w \geq 0.6$ mm and $T \geq 70$°C (see **Figure 5b**), indicating that a concave deformation changed to a swelling shape. Upon firing, the organic binders burnt out of the laminates and the contained glass phase melted to dissolve ceramic particles. As pores in the laminate were filled by viscous flow of glass, the resulting densification led to large shrinkage at the planar direction. It may suggest that such a driving force of the shrinkage stretched the concave cavity walls, formed by the lamination, against their own gravity during the densification process. Such a stretch, so-called "drumhead" effect [43], recovered the embedded cavities from their concave deformation, and even resulted in a slight outward bulging. We speculate this deformation recovery may result in increased local stress distribution at edge of the suspending parts, however, no crack in this region was observed in all samples.

The results of HL2K samples showed a different trend from the DP951 ones, that the deformation of the cavity walls developed further (see **Figure 5f&h**) after firing in all tested conditions, which was different from observations in previous studies[23]. For example, the deflection of embedded cavities with w = 1.2 mm were almost 5 times more than these ones measured after the lamination at either T = 90°C and P = 2 MPa or T = 70°C and P = 8 MPa shown in **Figure 5f&h**. Overall, we suggest that the deformation of embedded cavities in HL2K is promoted by the firing process because of the mutually constraining between its outer layers and refractory layer.

A straightforward way to improve the deformation is to increase the thickness of the embedded cavity walls, in other word, enhancing the mechanical strength of the suspending part over the embedded cavities in the laminate. The deflection of cavities in fired HL2K becomes less with the increasing thickness of the cavity walls **(see Figure S2).** For example, for the cavity with a width of 1.2 mm, the deflection of the cavity wall resulted in ~15 μm, much smaller than the one with the cover that has a green state thickness of 133 μm thick, produced under the same process conditions. The work also extended to the use of three HL2K green tapes as the cover layer, in which no noticeable deformation of embedded cavities was found. However, this approach may become constrained by the raw material cost, the device dimension or some situations that a thin cover layer is required, e.g. thermographic characterization[21].

Based on these results, we found that the standard firing process for both cases were still applicable in the use of such a lamination method. The optimized low-pressure lamination, for both DP951 and HL2K, in the multi-step lamination process was summarized as $T = 60 - 70$°C and $P = 2$ MPa for having minimal deformation of embedded cavities. Besides, we would not recommend T = 40°C for the fabrication of both cases, as small delamination was found in some of fired DP951 or HL2K samples (see **Figure 6a&b**). **Figure 6c&d** shows the cross-section of testing samples with embedded cavities that were fabricated by the optimized processing parameters. No noticeable deformation was observed at the cavity walls, for DP951 or HL2K cases, even within embedded channels more than 3 mm wide. Particularly, DP951 shows much less deformation in fabricating embedded cavities due to its "drumhead" effect.

Aside from the deformation, the bonding of LTCC tapes is another important measure to the quality of the microreactor fabrication. At green state, such joining in the LTCC laminates is mainly dependent of the contained organic binders as well as the mechanical bonding[13]. As stated previously, both lamination pressure and temperature enhance the organic binder's fluidity to improve the tape joining. Especially, the lamination pressure must be higher than such a yield point of the organic binder to achieve good lamination. However, people have to be aware that too high lamination pressure would damage the embedded fluidic structure. Thus, a trade-off between the lamination process and the good quality of LTCC tape joining must be found. Here, due to difficulties in fabricating cross-sections, we were unable to study the joining of LTCC samples in green state, which might indicate the unfired bonding strength is low. Another bonding mechanism occurs at the firing stage: the organic contents burn out and the glass melts to form viscous flow and bonds ceramics together as monolithic pieces [13, 23]. We did succeed in obtaining the cross-section of these LTCC samples that are laminated with optimized process values and fired under standard conditions; no any delamination or large pore formation were observed (see Figure S3). As compared to the DP951 samples that appeared more monolithic bonding, the HL2K ones showed a kind of layered structure that was mainly due to the tape's sandwiched structure[31]. It has been evidenced by Jurkow [23] that high porosity is obtained in such layered structure of fired HL2K samples. This might be resulted from HL2K's self-constraint sintering behavior and/or the improper burnt-out of organics. Nevertheless, with using our developed process, embedded fluidic structures can be obtained with good quality of bonding and very limited deformation. It is very feasible for developing microreactors that usually have fluidic channels at within sub-mm scales.

Applications

Disk-shape passive micromixers

A LTCC-based disk-shaped micro-scale passive mixer has been developed successfully for the first time through using our developed LTCC microfabrication process. This micromixer is designed as a single-channel continuous microreactor with a "T" type mixing entrance. In a fluidic channel, there is a series of tangential mixing channels in disk-shape, which has recirculation zones on each side of the structure with major throughput at the center. Such a mixing design could effectively enhance the convective back-mixing of reactant fluids and was reported in several stainless steel-based microreactors for pharmaceutical productions[44]. Comparing with alloy-based microreactors, LTCC ones have lower thermal conductivity, which would be greatly beneficial for studying the fluidic mixing of exothermic reactions, as the thermal influence from the reactor bodies are very minimal. Using our developed laser cutting and multi-step lamination processes, LTCC micromixers, made of DP951 LTCC tapes, were successfully developed with embedded disk-shaped mixing fluidic structure. In the 30 mm long mixing channel, there were 8 disk-shape mixing structure with a diameter of 2.0 mm per each, as shown in **Figure 7**a. The top wall of the fluidic channel after firing was only 100 μm thin (not shown). The profilometric results of this cover indicated deformation in concave shape with a 20 μm deep at most for the embedded disk-shaped cavities, as compared with 500 μm high in fluidic channels (see **Figure 7**b). The dimensional deviation of the top cavity wall to the fluidic channels is only about 4%. A mixing of sulfuric acid (7.5 mol·L^{-1}) and pseudoionone (1.2

mol·L^{-1}) was used as a model reaction to examine the device's performance on basis of its quasi-instantaneous exothermic characteristic[21].

Continuous monitoring of a chemical reaction inside such small channels is generally challenging. Typically, the approach to use in our studies is rather qualitative, i.e. to characterize the reaction kinetics and thermodynamics, which in turn allows the design of a stable chemical process. In such cases, it is enough to monitor the conditions at the inlet and outlet of the reactors. In addition, with help of the thin top cover layer, an infrared thermographic method was able to visualize temperature profiles along the mixing channel. The results showed that the temperature reached its maximum at middle of the mixing channel (see **Figure 7**c), suggesting a good mixing happened there for a 0.47 m·s^{-1} flow rate of feedstock (Re ≈ 75)[45]. This application proves our LTCC microfabrication process as a fast, inexpensive and flexible method for developing liquid phase continuous flow channel-reactors.

Staggered herringbone micromixers

Recently, a chaotic mixing layout, so-called staggered herringbone structure, has been proposed for an efficient mixing at very low Reynolds number (Re < 100) in continuous-flow microchannel reactors[46]. Such a mixer contains series of grooves built on the bottom side of fluidic channels. By altering directions of such grooves, the structure can enforce flows to be folded successively on the top of each other and thus produce effective chaotic advection for mixing the fluids. We have been exclusively reported LTCC-based microreactors with integrated staggered herringbones for fluidic mixing applications. The optimized laser micromaching and multi-step lamination processes allowed a production of 96 μm wide grooves at the bottom channel walls in the microreactors (see **Figure 8**a). Using the same model reaction as described above, the thermographic results demonstrated that an effective mixing occurred at 18 mm away from the mixing point in a 30 mm long fluidic channel (see **Figure 8**b), while the *Re* = 20 for feedstock (flow rate 0.12 m·s^{-1}). Comparing with ones without staggered herringbones, the mixing performance was greatly improved in these LTCC microreactors for such a low feeding rate[21].

Multiple-injections microreactors for ionone production

The liquid-phase cyclization of pseudoionone is an important chemical process for producing α- and β-ionone that are extensively used in pharmaceutical and fragrance industries[47]. However such a process takes place only in the presence of sulfuric acid. This is a quasi-instantaneous exothermic reaction. Due to the very fast kinetics, mixing of sulfuric acid and peudoionone plays a crucial role since the acid concentrations influence product distribution and the global transformation rate. Undesirable hot spots can be easily formed in the microreactor, leading to low yields of ionones and their polymerization. The latter one in turn can produce more exothermic reactions and results in clogging fluidic channels[48]. Even using microreactors with high thermal conductive materials, the overshooting temperature at the mixing point cannot be avoided. Therefore, concepts of multiple-injection and heat exchangers were proposed for better temperature control in continuous-flow microreactors for the ionones production[21]. **Figure 9a** depicts the design of our developed LTCC multiple-injection microreactors. The device consisted of two fluidic parts, totally 7 functional layers: (a) the upper reaction part had three injection inlets and corresponding fluidic channels,

each of which contained a series of staggered herringbone mixing channels and an interconnection channel; (b) the bottom part enclosed three individual cooling channels (8.8 mm in width per each) running isopropanol coolants beneath the reaction channels.

The temperature profile of the chemical reaction was experimentally visualized by the infrared thermography. In the use of single injection, the temperature rose up significantly more than 25% of the adiabatic temperature in the herringbone mixing channel (see **Figure 9b**). Contrastively, the temperature raise was only 12% of the adiabatic temperature using the multiple-injection method with three injection points. Moreover, the temperature in the interconnection channels was able to be cooled more efficiently by the integrated heat-exchangers due to the large heat exchanging area at channel wall (see **Figure 9**b). The overall reaction temperature was well-controlled in the range of 30 – 60°C with helps of the gradual mixing of reactants along the herringbone mixer and the active cooling. Consequently, a combined yield of α-ionone and β-ionone over 98% was achieved in the device, using a total 0.18 $m \cdot s^{-1}$ flow rate of 7.5 $mol \cdot L^{-1}$ sulfuric acid and 1.5 $mol \cdot L^{-1}$ pseudoionone. This development well proves the extensive capability of the LTCC microfabrication process for developing complex meso-scale microreactors, which are able to incorporate various functional fluidic structures together as one monolithic piece, for performing chemically harsh and exothermic reactions, especially for these ones that are not dependent of the intrinsic kinetics but controlled by the mixing of chemical reactants.

Further applications of such LTCC-based microreactors may be found in the laboratory as well as in the large-scale chemical production. In the former case, this kind of microreactor can be used to generate understanding regarding a specific reaction (kinetics and thermodynamics). Especially, monitoring tools can be integrated directly into the microreactor channels, for instance, temperature and pressure sensing probes, which opens a wide field of opportunities to this type of devices. More specifically, one can use the hydrophilic wall properties (see Figure S4) to create droplets of organic compounds in an aqueous phase, allowing precise kinetic models of any organic reaction to be established in a similar fashion as described by Kashid et al48. The use of the LTCC microreactor in production is rather limited to quasi-instantaneous reactions, as the maximum volume provided with this kind of microreactor is in the range of milliliters. The most prominent examples for this case are organometallic reactions such as with Grignard reagents.

High-temperature microreactors for hydrogen production

Another good example of LTCC microreactors made by our developed LTCC microfabrication process is the portable high-temperature (> 400°C) LTCC hydrogen generator[20]. In this work, a catalytic partial oxidation of propane for producing hydrogen is used as the model reaction. Ru-containing nanoparticles on inert ceramic supporters were applied as catalysts (see Figure 10c).

As shown in (see Figure 10a), the microreactor had a slender bridge design and contained two working zones: (i) a hot zone to perform the chemical reaction, and (ii) a cold zone, where standard fluidic and electrical interconnections were able to be used without concerns of thermal stability. The integrated thick-film heaters (see Figure 10b) enabled to heat up the hot zone above 600°C, while the bridge structure provided an effective thermal decoupling to remain the cold zone under 80°C. Several fluidic structures with varied functionalities were able to be integrated in the hot zone:

(a) gas distributors were placed at entrance of the packed bed for better distributed inflows (see Figure 10d); (b) a packed-bed chamber had a size of 19.7 × 12.0 × 2.0 mm^3, with a catalyst loading window, for performing the catalytic partial oxidation (see Figure 10e); (c) a middle layer with embedded thick-film heaters separated the packed bed and exit chambers and provided thermal energy to the reaction locally, in which the heaters also functioned as temperature sensors for monitoring the chemical process (see Figure 10b); (d) an exit outlet chamber below the middle layer connected the packed bed to the cold-zone (see Figure 10e). Using our developed microfabrication strategy, microreactors with these fluidic structures were able to be fabricated with very minimal deformation, especially the gas distributors with multiple micron-sized honeycomb channels and large suspended reactor walls over the reaction chamber (see Figure 10b,d&e). Using such a bridge structure design (see Figure 10a), the LTCC microreactor enabled to achieve two working zones in one device at different temperature. The infrared thermographic result (see Figure 10f) indicated that the "hot" area for chemical reactions reached an average temperature of 400°C, heated by the embedded thick-film heaters, and the "cold" area kept below 100°C, where standard electrical/fluidic interconnections can be used for integrating processing monitoring tools, e.g. temperature and pressure sensors. More information on such thermal design and characterization can be found in our previous work [20].

This device, fed by 0.01 $m \cdot s^{-1}$ of propane and air mixture, achieved a combined yield of hydrogen and carbon monoxide up to 71% at 642°C of reactor operating temperature. The overall reaction lasted for more than 5 hours, and no any structural or electronic failure observed in the devices, showing that the high resistance of LTCC microreactors against high temperature (> 400°C) environment. More important, the development not only proves the versatility of LTCC fluidic fabrication for constructing complex fluidic channels, but also demonstrates multi-functionalities with integrated heating and temperature sensing abilities, which could be very beneficial to the accurate process control and automation.

Conclusions

A novel low-temperature co-fired ceramic microfabrication process was developed to integrate various intact and complex fluidic channels into microreactors that were able to perform chemical reactions under harsh conditions. Especially the material stability test showed highly chemical resistance of fired LTCC against concentrated basic and acid solutions.

The fabrication method consisted of an optimized laser micromachining, a multi-step lamination and a standard firing step. Out studied showed both laser processing parameters and LTCC green tapes had strong influences on structuring fine fluidic features. Staggered herringbone structures, at the scale of 100 μm, were for the first time fabricated successfully in the LTCC green tapes. For the multi-step lamination, our profiliometic results and cross-section examination showed that mm-scale fluidic channels were able to be integrated into meso-scale microreactors without any sagging or collapsing. Limited deformation was only found in these cases involved with thin fluidic wall (< 120 μm) or large suspending layers (∽ 230 mm^2). More important, this process did not require any

additional chemical assistance or sacrificial volume materials, and feasible for the use of standard manufacturing firing process.

Various microreactors based on our developed LTCC fabrication strategy were demonstrated exclusively in application of high-temperature and chemically harsh reactions:

1) A passive disk-shaped tangential micromixer was developed with a thin top fluidic wall (~ 100 μm) for thermographic characterization of exothermic mixing reactions.
2) A micromixer with incorporated staggered herringbone mixing structure was achieved, which delivered an efficient mixing of 7.5 mol/L sulfuric acid and 1.2 mol/L pseudoionone for low Reynolds number of feedstock (Re ≈ 20).
3) A multi-injection microreactor was demonstrated for the ionones production, in which the staggered herringbone mixing structure, the multiple injection fluidic channels and the liquid phase heat exchangers were incorporated successfully. The device led to a combined yield of α-ionone and β-ionone over 98% from the cyclization of pseudoionone at a total flow rate of 0.18 $m \cdot s^{-1}$.
4) A high temperature microreactor for portable hydrogen production was developed with integrated thick-film heating elements and a catalytic packed bed. The device was able to be self-heated up over 600°C in specific areas, while the other parts remained at low temperature (< 100°C) that standard fluidic and electrical connections were used. The microreactor delivered a combined yield of hydrogen and carbon monoxide as high as 71% from 0.01 $m \cdot s^{-1}$ feed of air and propane mixture at 642°C.

Our advancements largely reduce the microreactor development cycle and simplify their fabrication process, especially in comparison with silicon-based microfabrication techniques. It is providing a promising solution to a simple, cheap and fast manufacturing of ceramic-based microreactor systems.

Acknowledgement

The authors would like to thank the Swiss National Science Foundation (contract number: 200021_143424) and the 7th European Framework program COPIRIDE project (contract number: CP-IP 228853-2) for the financial support.

Reference

1. Batoul Ahmed-Omer, Johan C. Brandt and Thomas Wirth, *Organic & Biomolecular Chemistry*, 2007, 5, 733-740.
2. Thomas Wirth, *Microreactors in Organic Chemistry and Catalysis*, Wiley. com, 2013.
3. R. Knitter, D. Göhring, P. Risthaus and J. Haußelt, *Microsystem Technologies*, 2001, 7, 85-90.
4. J. Vican, B. F. Gajdeczko and F. L. Dryer, *Proceedings of the Combustion Institute*, 2002, 29, 909-916.
5. F. Meschke, G. Riebler, V. Hessel, J. Schürer and T. Baier, *Chemical Engineering & Technology*, 2005, 28, 465-473.
6. Christian, M. Mitchell, D. P. Kim and P. J. A. Kenis, *Journal of Catalysis*, 2006, 241, 235-242.
7. Takashi Okamasa, Gwang-Goo Lee, Yuji Suzuki, Nobuhide Kasagi and Shin Matsuda, *Journal of Micromechanics and Microengineering*, 2006, 16, S198-S205.
8. Marko Hrovat, Darko Belavic, Gregor Dolanc, Primoz Fajdiga, Marina Santo-Zarnik, Janez Holc, Mitja Jerlah, Kostja Makarovic, Stanko Hocevar and Iztok Stegel, *Journal of Microelectronics Electronic Components and Materials*, 2011, 41, 171-178.
9. Darko Belavič, Marko Hrovat, Gregor Dolanc, Marina Santo Zarnik, Janez Holc and Kostja Makarovič, *Radioenineering*, 2012, 21, 195-200.
10. Cynthia S. Martínez-Cisneros, Sara Gómez-de Pedro, Mar Puyol, Joan García-García and Julián Alonso-Chamarro, *Chemical Engineering Journal*, 2012, 211-212, 432-441.
11. Caroline Jacq, Thomas Maeder and Peter Ryser, *Sadhana*, 2009, 34, 677-687.
12. Christian Bienert and Andreas Roosen, *Journal of the European Ceramic Society*, 2010, 30, 369-374.
13. Yoshihiko Imanaka, *Multilayered low-temperature co-fired ceramics (LTCC) technology*, Springer US, Boston USA, 2004.
14. Núria Ibáñez-García, Julián Alonso, Cynthia S. Martínez-Cisneros and Francisco Valdés, *TrAC Trends in Analytical Chemistry*, 2008, 27, 24-33.
15. Christian Atzlesberger and Walter Smetana, presented in part at the 30th International Spring Seminar on Electronics Technology, Cluj-Napoca, Romania, 2007.
16. Karin Schindler and Andreas Roosen, *Journal of the European Ceramic Society*, 2009, 29, 899-904.
17. Stefan P Wilhelm, Robert W Kay, Mazher I Mohammed, Yves Lacrotte and Marc PY Desmulliez, *Microsystem Technologies*, 2013, 19, 801-807.
18. Walter Smetana, Bruno Balluch, Günther Stangl, Sigrid Lüftl and Sabine Seidler, *Microelectronics Reliability*, 2009, 49, 592-599.
19. Karol Malecha, Dominik Jurków and Leszek J. Golonka, *Journal of Micromechanics and Microengineering*, 2009, 19, 065022-065022.
20. Bo Jiang, Alejandro J. Santis-Alvarez, Pual Muralt, D. Poulikakos and Thomas Maeder, *Journal of Power Sources, in press*, 2014.
21. Julien Haber, Bo Jiang, Thomas Maeder, Albert Renken and Lioubov Kiwi-Minsker, *Green Processing and Synthesis*, 2013, 2, 435-449.
22. Karol Malecha, Leszek J. Golonka, Jerzy Bałdyga, Magdalena Jasińska and Paweł Sobieszuk, *Sensors and Actuators B: Chemical*, 2009, 143, 400-413.
23. Dominik Jurków and Leszek Golonka, *Journal of the European Ceramic Society*, 2012, 32, 2431-2441.
24. Andreas Roosen, *Journal of the European Ceramic Society*, 2001, 21, 1993-1996.
25. Dominik Jurków and Leszek Golonka, *International Journal of Applied Ceramic Technology*, 2010, 7, 814-820.
26. Jennifer a Lewis, *Annual Review of Materials Science*, 1997, 27, 147-173.

27. H. Birol, T. Maeder, C. Jacq, S. Straessler and P. Ryser, *International Journal of Applied Ceramic Technology*, 2005, 2, 364-373.
28. Karol Malecha, Thomas Maeder and Caroline Jacq, *Journal of the European Ceramic Society*, 2012, 32, 3277-3286.
29. Eszter Horváth and Gábor Harsányi, *Periodica Polytechnica Electrical Engineering*, 2010, 54, 79-79.
30. W Kinzy Jones, Yanqing Liu, Brooks Larsen, PENG Wang and Marc Zampino, *The International Journal of Microcircuits and Electronic Packaging*, 2000, 23, 469-473.
31. Torsten Rabe, Wolfgang A. Schiller, Thomas Hochheimer, Christina Modes and Annette Kipka, *International Journal of Applied Ceramic Technology*, 2005, 2, 374-382.
32. DuPont 951 LTCC Green Tape™, E.I. DuPont de Nemours and Company, 2001.
33. HERALOCK™ HL2000 Materials System, Heraeus, Circuit Materials Division, 2012, pp. 1-14.
34. Krzysztof M. Nowak, Howard J. Baker and Denis R. Hall, *Applied Physics A*, 2010, 103, 1033-1046.
35. Jijun Zhu and Winco KC Yung, *The International Journal of Advanced Manufacturing Technology*, 2009, 42, 696-702.
36. M. Farhan Shafique, Andrew Laister, Michael Clark, Robert E. Miles and Ian D. Robertson, *Journal of the European Ceramic Society*, 2011, 31, 2199-2204.
37. Wenli Zhang and Richard E. Eitel, *International Journal of Applied Ceramic Technology*, 2012, 9, 60-66.
38. Thomas Maeder, Caroline Jacq, Yannick Fournier, Wassim Hraiz and Peter Ryser, presented in part at the 17th European Microelectronics & Packaging Conference (EMPC), Rimini, Italy, 2009.
39. Marion Gemeinert, Doktor-Ingenieur, der Technischen Universität Bergakademie Freiberg, 2009.
40. Jaroslaw Kita, Andrzej Dziedzic, Leszek J. Golonka and Tomasz Zawada, *Microelectronics International*, 2002, 19, 14-18.
41. B Balluch, S Lüftl, S Seidler and W Smetana, presented in part at the International Conference of IMAPS Poland Chapter, Pultusk, Poland, 2008.
42. LE Khoong, YM Tan and YC Lam, *Journal of the European Ceramic Society*, 2009, 29, 2737-2745.
43. Yannick Fournier, Thomas Maeder, Grégoire Boutinard-Rouelle, Aurélie Barras, Nicolas Craquelin and Peter Ryser, *Sensors*, 2010, 10, 11156-11173.
44. Norbert Kockmann, Michael Gottsponer and Dominique M. Roberge, *Chemical Engineering Journal*, 2011, 167, 718-726.
45. Julien Haber, Bo Jiang, Navid Borhani, Thomas Maeder, John Richard Thome, Albert Renken and Lioubov Kiwi, presented in part at the 9th European Congress of Chemical Engineering (ECCE), The Hague, Holland, 2013.
46. Nam-Trung Nguyen and Zhigang Wu, *Journal of Micromechanics and Microengineering*, 2005, 15, R1-R16.
47. V. K. Díez, B. J. Marcos, C. R. Apesteguía and J. I. Di Cosimo, *Applied Catalysis A: General*, 2009, 358, 95-102.
48. Madhvanand N. Kashid, Igor Yuranov, Pauline Raspail, Petra Prechtl, Jacques Membrez, Albert Renken and Lioubov Kiwi-Minsker, *Industrial & Engineering Chemistry Research*, 2011, 50, 7920-7926.

Figures

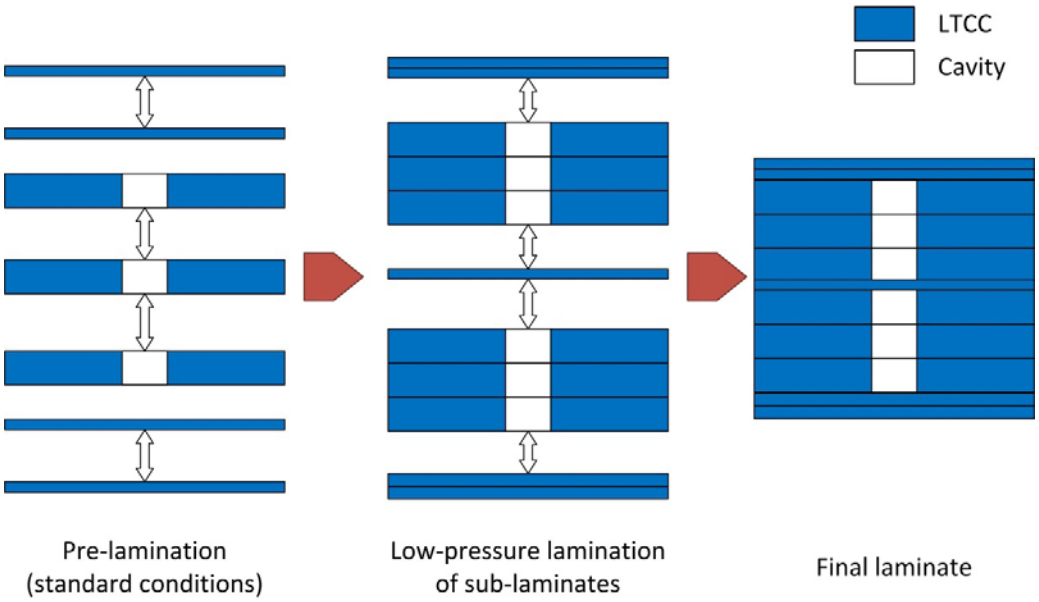

Figure 1. A schematic view of the multi-step lamination process

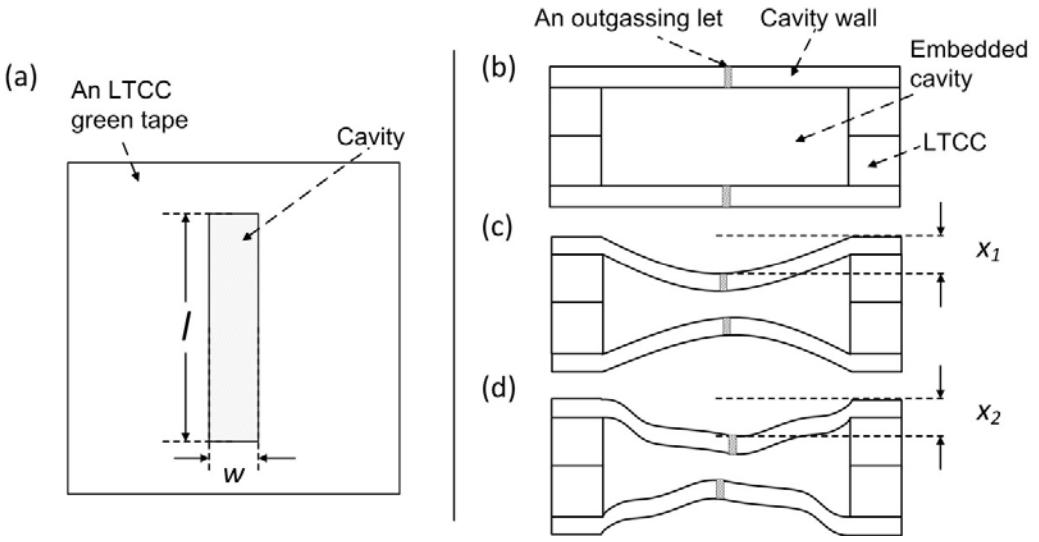

Figure 2 Schematic views of the multi-step lamination optimization test: (a) a LTCC green tape with a testing cavity; (b) the cross-section of laminates with embedded cavities before lamination; (c) the deflection definition of samples after lamination; and (d) the deflection definition of samples after firing.

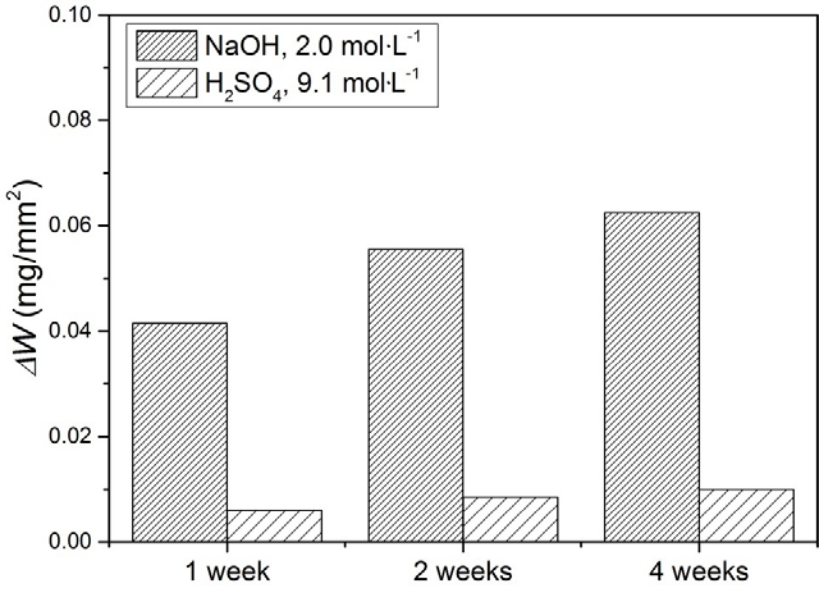

Figure 3 Chemical stability results of fired HL2K LTCC in 2.0 mol·L^{-1} of sodium hydroxide (NaOH) and 9.1 mol·L^{-1} of sulfuric acid (H_2SO_4) aqueous solution

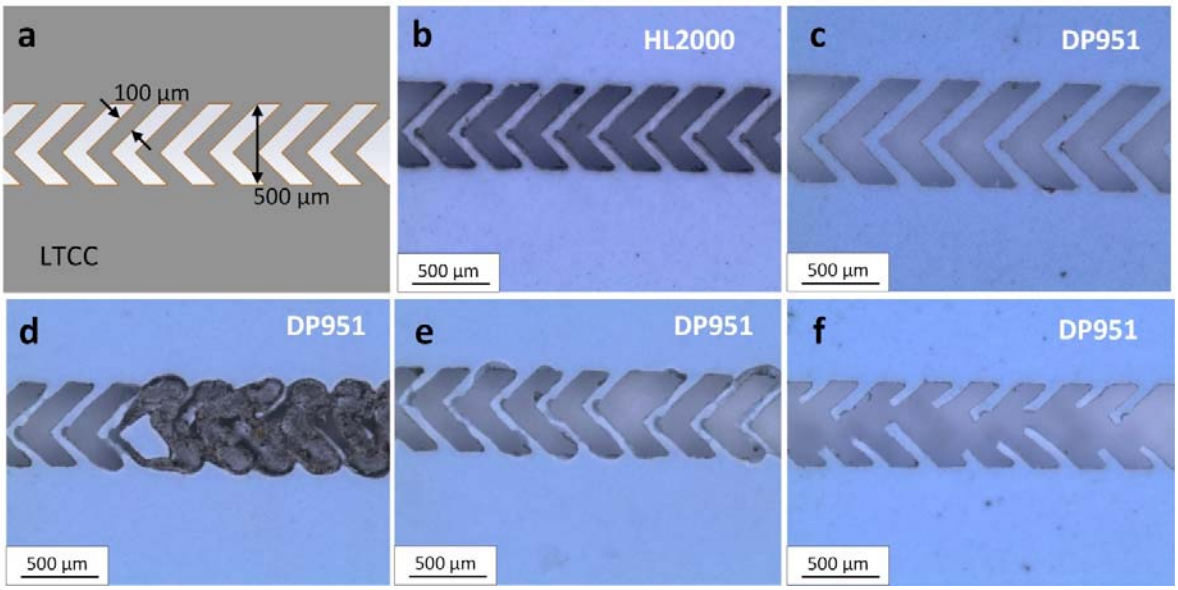

Figure 4 (a) A schematic of herringbone fluidic structure layout; (b) HL2K and (c) DP951 of laser-machined herringbone structure with using optimized laser process. Optical images of structure failures in DP951 tapes due to inadequate laser process parameters: (d) incomplete laser cut, (e) side wall bulging and (f) damaged herringbone structures.

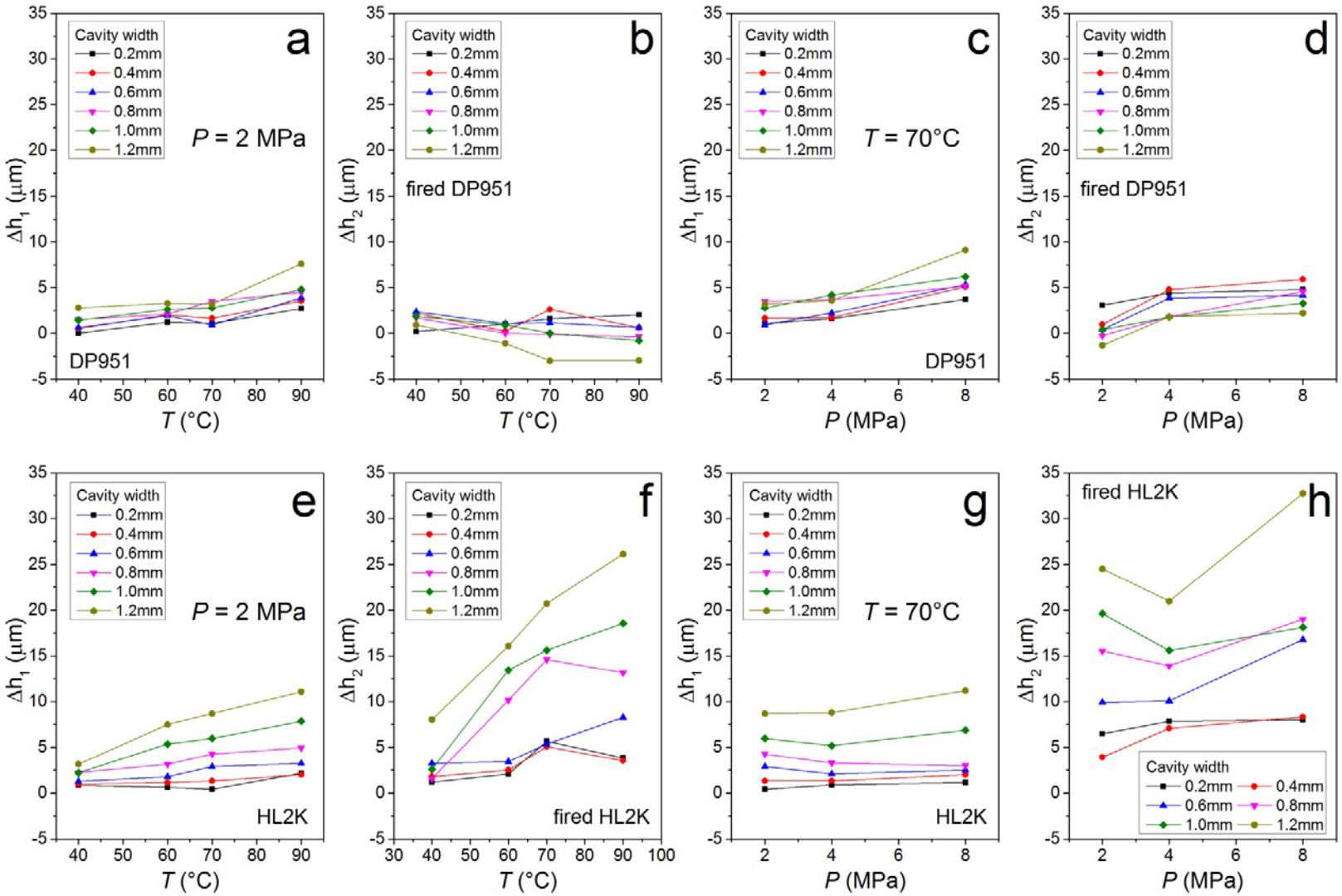

Figure 5 Deflection results of DP951 testing fluidic structure: samples (a) after lamination and (b) fired at varied lamination temperature; samples (c) after lamination and (d) fired at varied lamination pressure. Deflection results of HL2K testing fluidic structure: samples (e) after lamination and (f) fired at varied lamination temperature; samples (g) after lamination and (h) fired at varied lamination pressure.

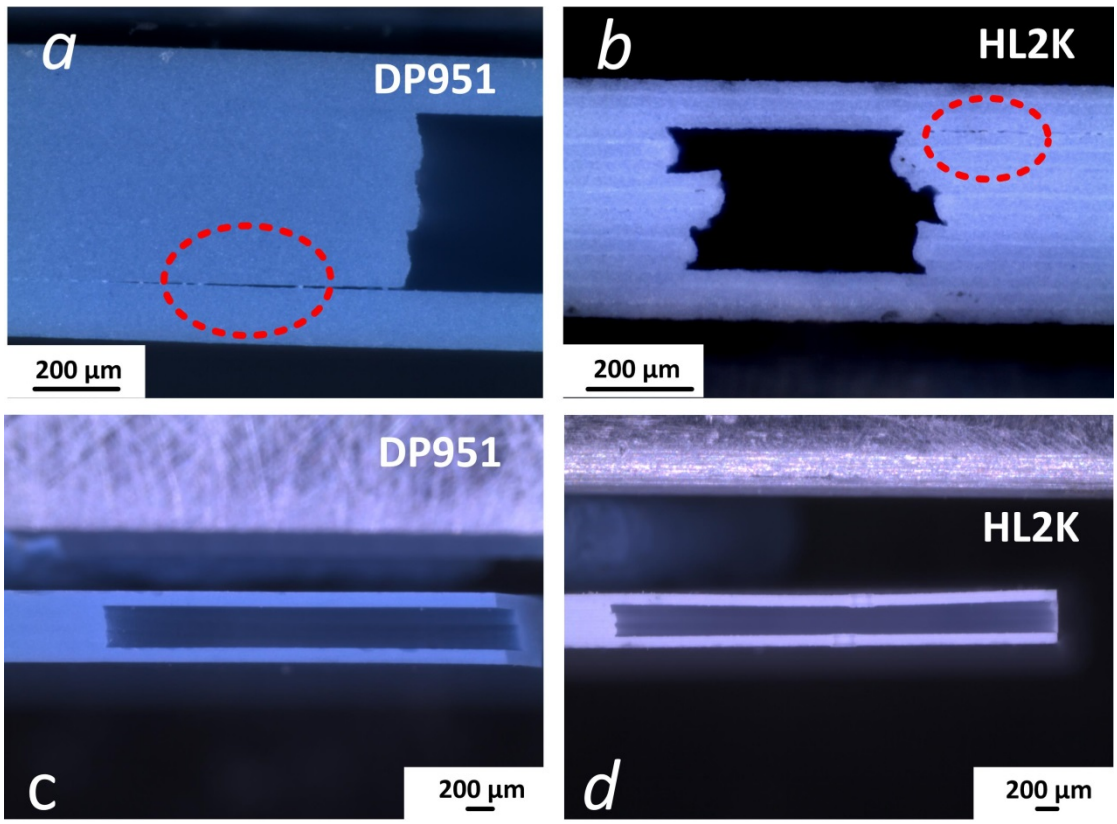

Figure 6 Optical images at cross-section of fired LTCC with embedded cavities: delamination shown in red dash lines for (a) DP951 and (b) HL2K samples using T = 40°C and P = 2 MPa; A half of 5.0 mm wide cavities shown in (c) DP951 and (d) HL2K using optimized low-pressure lamination process (T = 70°C, P = 2 MPa).

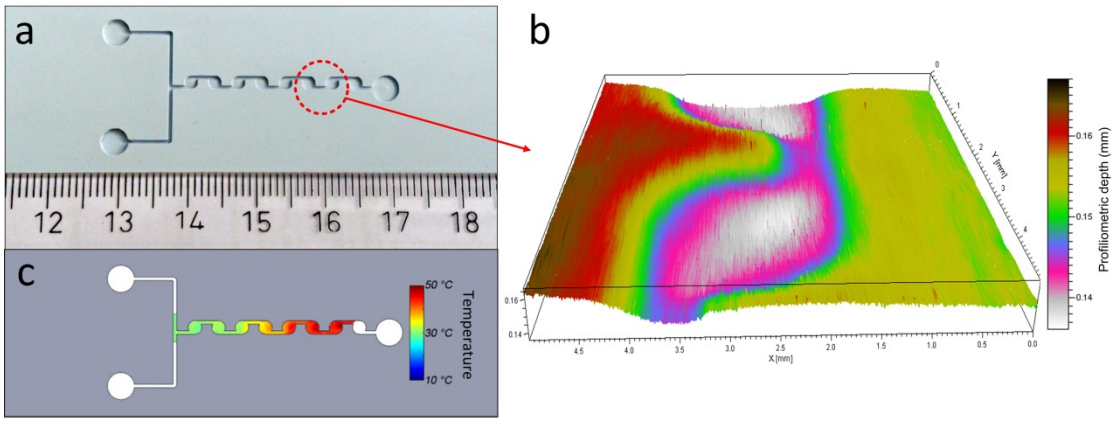

Figure 7 A disk-shaped LTCC micromixer for chemical mixing applications: (a) A top-view of the LTCC micromixer without the top cover; (b) a profilometric result of the LTCC micromixer with the top cover (thickness ≈ 100 μm); (c) an infrared result in the disk shaped microchannel mixing of sulfuric acid (7.5 mol·L^{-1}) and pseudoionone (1.2 mol·L^{-1}) at high flow rate (0.47 m·s^{-1}).

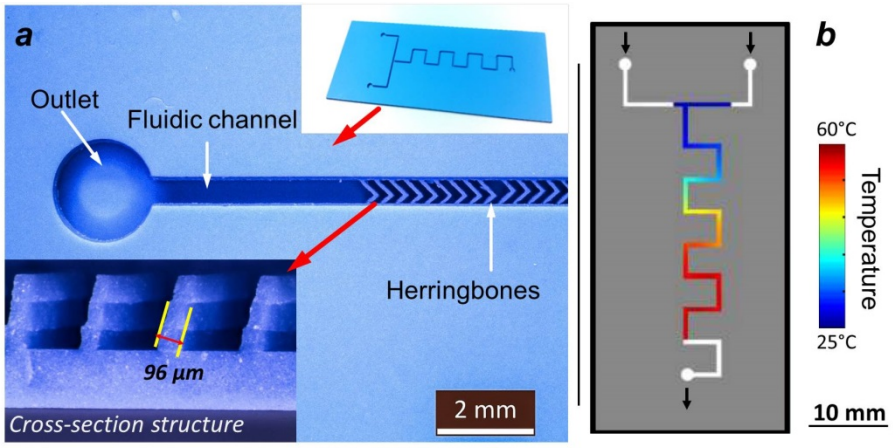

Figure 8 An LTCC microreactor (without a top cover) with herringbone structures for chemical mixing applications: (a) microstructural images of a fabricated microreactor containing staggered herringbone structure in a fluidic channel; (b) an infrared result in the microreactor channels mixing of sulfuric acid (7.5 mol·L^{-1}) and pseudoionone (1.2 mol·L^{-1}) at low flow rate (0.12 m·s^{-1}).

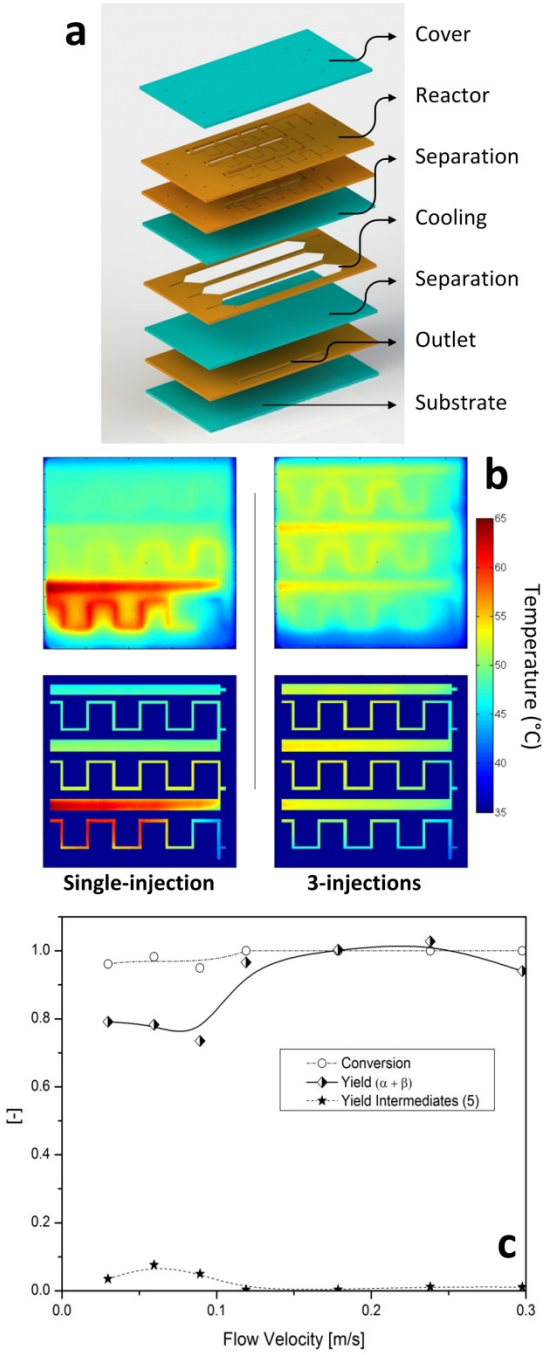

Figure 9 A multiple-injections LTCC microreactor with integrated herringbone mixers and cooling function for ionone production: (a) a schematic view of a multiple-injections LTCC microreactor; (b) thermographic results of the microreactor running under the single-injection and 3-injections modes; (c) chemical analysis at varied flow rate with using the 3-injections operation.

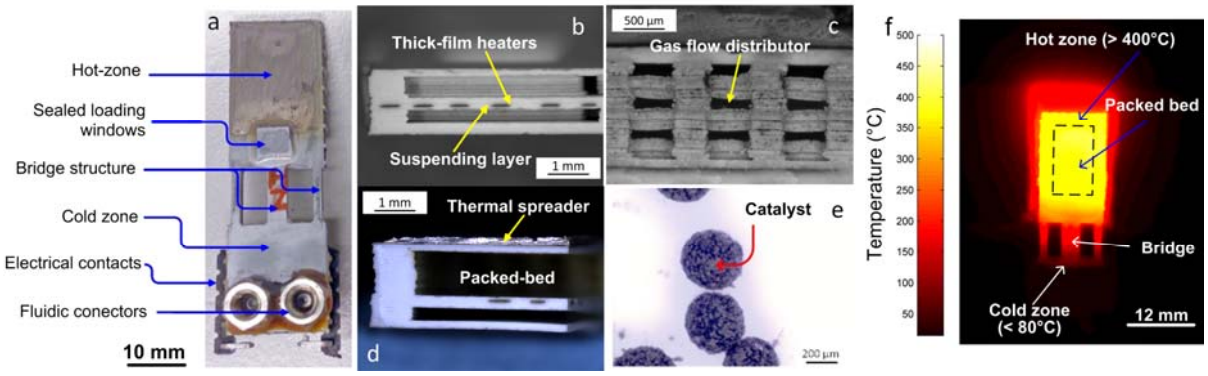

Figure 10 An LTCC microreactor for high temperature (> 400°C) hydrogen production via partial oxidation of propane: (a) a photo of the LTCC microreactor; (b), (d) and (c) structural images of fluidic channels at the cross-section of the microreactor; (e) a photo of the used catalyst; (f) an infrared image of the LTCC microreactor operating at an average temperature of 400°C.

Equations

$$\Delta W = \frac{W_0 - W_x}{S}, (x = 1, 2, 4) \quad \textbf{Equation 1}$$

$$\Delta h_1 = x_1 \quad \textbf{Equation 2}$$

$$\Delta h_2 = x_2 - x_1 \quad \textbf{Equation 3}$$

Tables

Table 1 Process parameters of the low pressure lamination test

Lamination test	1	2	3	4	5	6	7
Temperature	70°C	70°C	70°C	40°C	60°C	70°C	90°C
Pressure	2MPa	4MPa	8MPa	2MPa	2MPa	2MPa	2MPa

Table 2 The firing process of tested LTCC materials

Firing profile	DP951	HL2K
Organics burnout	25°C to 400°C by 13 °C·min^{-1} 400°C to 600°C by 4.6 °C·min^{-1}	25°C to 100°C by 3°C·min^{-1} 100°C to 450°C by 2°C·min^{-1}
Ceramic sintering	600°C to 895°C by 7.1°C·min^{-1} 30 min dwell	450°C to 865°C by 8°C·min^{-1} 30 min dwell
Cooling	895°C to 50°C by 20.5°C·min^{-1}	865°C to 50°C by 10°C·min^{-1}

Supplemental information

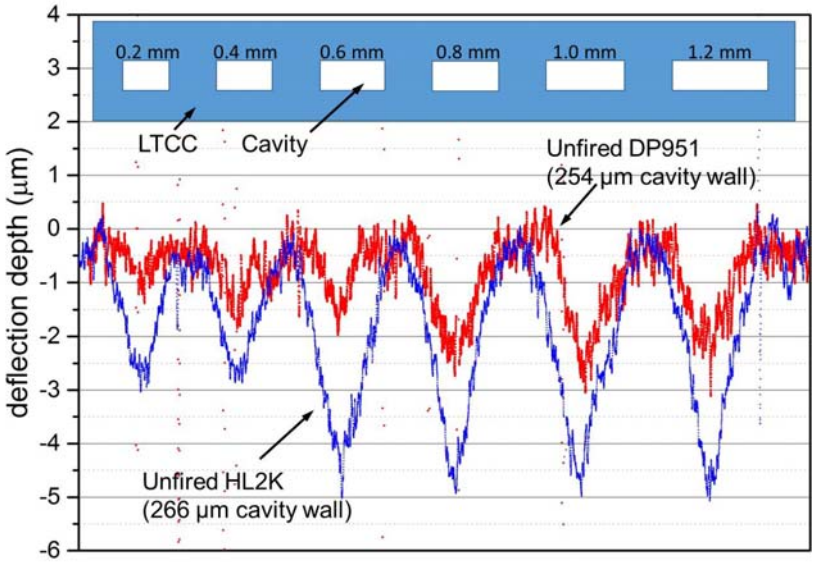

Figure S1 A comparison of deflection profile in laminated HL2K (266 µm, in blue) and DP951 (254 µm, in red) at green state with similar cavity wall thickness.

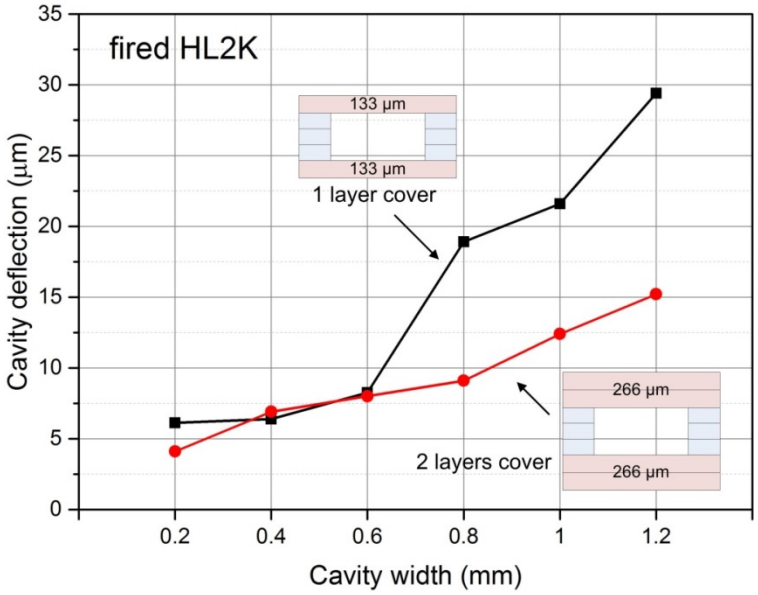

Figure S2 Cavity deflection results of fired HL2K samples with one (in black) and two (in red) cover layers

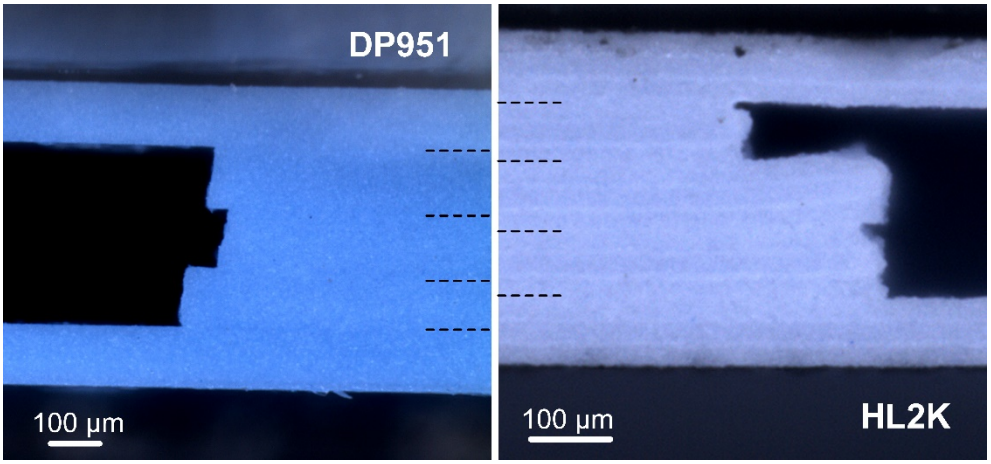

Figure S3 Cross-section images of LTCC DP951 (left) and HL2K (right) samples laminated under pressure of 2 MPa at 70°C and fired by their standard conditions. The dash lines indicate the layer of each LTCC tape.

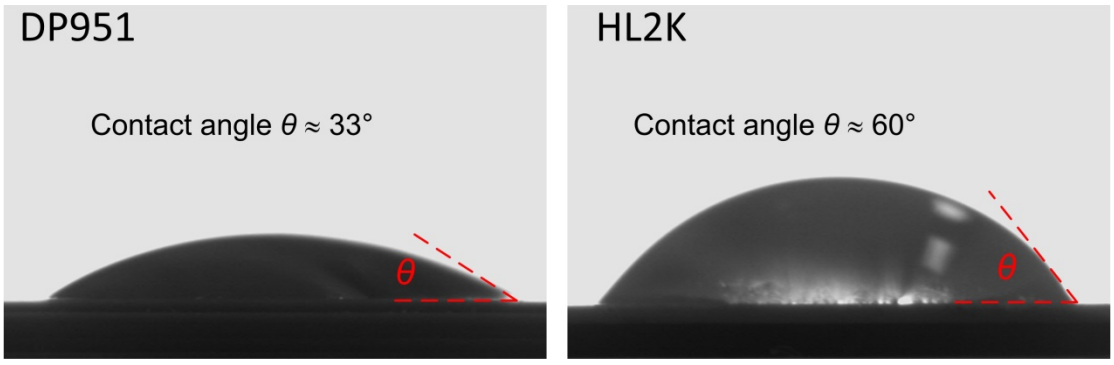

Figure S4 Contact angle results of fired DP951 (left) and HL2K (right) LTCC material using aqueous droplets.